Final Technical Report

PROJECT TITLE:	Mechanisms of Ultra-High Efficiency Chemical Suppressants
SERDP PROJECT IDENTIFIER:	NGP 2a2
RESEARCH CATEGORY:	6.2 Applied Research
AGENCY:	Navy
LAB:	Naval Research Laboratory

PI:

Dr. James Fleming (NRL)
Code 6185
Naval Research Laboratory
Washington, DC 20375-5342
phone: 202-767-2065
fax: 202-767-1716
fleming@code6185.nrl.navy.mil

co-PI:

Dr. Bradley A. Williams (NRL)
Code 6185
Naval Research Laboratory
Washington, DC 20375-5342
phone: 202-767-3583
fax: 202-767-1716
brad@code6185.nrl.navy.mil

THRUST AREA:	2A Mechanisms of Chemical Suppressants
PROJECT DATES:	April 1998 – May 2001
REPORT DATE:	October 1, 2003

Sponsored by:
The Department of Defense
Strategic Environmental Research and Development Program

TABLE OF CONTENTS

I. EXECUTIVE SUMMARY

A. TASK OBJECTIVES

The objective of this project was to determine how chemicals that are as or more efficient than Halon 1301 (CF_3Br) quench the various flames of military interest in order to identify high-efficiency chemical fire suppression agents as candidates for replacing Halon 1301. To answer this question, three specific tasks were undertaken, all based on an assessment of the behavior of prototype "superagent" fire suppressants such as iron pentacarbonyl. These were: (1) understand key chemical reactions or processes of combustion which are affected by "superagent" suppressants and how these reactions or processes differ from those important for fire suppression by Halon 1301; (2) determine the requirements for (and partitioning of) the contributions of a suppressant's chemical and physical interactions with flames, leading to guidelines for suppression systems; (3) determine minimum properties for a "superagent" suppressant.

B. TECHNICAL PROBLEMS

Superagents are typically metal or alkali metal compounds that typically exist as liquids or solids at room temperature. The evaluation of these compounds under the same conditions for comparison purposes is often difficult if not impossible. Flame configurations that are very amenable to the study of gas-phase suppression (e.g cup burner flames) are difficult or totally not appropriate for studying condensed phase suppression compounds. Also, because of their very high efficiencies, superagents compounds are required only in very small quantities. Controlling the delivery of small amounts of condensed phase compounds and the subsequent monitoring of these compound under flame conditions are challenges.

C. GENERAL METHODOLOGY

Specific plans of the project included the following: develop list of suppressants (current NGP efforts, scientific literature, mechanistic insight gained from project) for compounds to investigate; select compounds for (a) physical suppression, (b) efficient chemical suppression, and (c) combined mechanism of suppression; examine flames in several configurations including non-premixed counterflow and premixed Bunsen flames; quantify additive effect on extinction strain rate in non-premixed counterflow flames and burning velocity reduction in premixed flames; characterize flame structure (flame species and temperature profiles) as function of additive concentration and strain rate; measure flow fields using (LDV) and/or (PIV); develop required chemical kinetic mechanisms; model inhibited flames using existing flame codes; compare flame structure modeling results to experimental measurements; provide systematic method for identifying new candidate suppressants based on mechanistic knowledge; and develop list of such chemicals.

D. TECHNICAL RESULTS

- Burning velocity of premixed flames seeded with small (< 0.5 micron diameter) water drops carried out to determine potential for introducing non-gaseous agents into flames.
- Burning velocity reduction of methane/air premixed flames agreed with theoretical maximum thermal effect of water. Total evaporation of drops established by light scattering.
- Burning velocity reduction of premixed methane/air flames by added alkali (sodium hydroxide solution) exhibit either (i) no significant reduction over pure water drops or (ii) flames could not be stabilized. Behavior consistent with the complete evaporation of drops in the various flames.
- Suppression effectiveness of efficient chemical inhibitors existing as liquids or solids at room temperature (requiring vaporization or decomposition) depends strongly on residence time and thus flame geometry (premixed versus non-premixed, counterflow versus co-flow) even for very small particle/drop sizes.
- A kinetic model was constructed and computationally evaluated for tin. The calculated suppression concentrations (based on tetramethyltin) are an order of magnitude higher than for potassium, iron, or manganese.
- Extinction strain rate calculations for methane/air counterflow non-premixed flames inhibited by dimethyl methylphosphonate (DMMP) agree with experimental data of Fisher et. al.(Cornell). Numerical results demonstrate a "strong saturation" effect for DMMP.
- Modeling calculations using assembled manganese kinetic mechanism show similar effectiveness for MMT(methylcyclopentadienyl manganese tricarbonyl) and monomanganese-pentacarbonyl. The estimated efficiency is 5-7 times less than that for Fe(CO)5. Uncertainties do exist in the estimation of the rate constants; the possibility exists that Mn compound suppression effectiveness could be higher than estimated.
- Modeling studies show that the behavior for bromine (as expressed by CF_3Br) behavior is not typical of highly efficient catalytic suppressants; the use of CF_3Br as a "baseline" for inhibitor mechanistic comparisons must be done with care.
- Modeling studies were carried out to compare Br (as provided by CF_3Br) to efficient catalytic scavengers (iron pentacarbonyl and sodium hydroxide), inert thermal agents (CF_4 and N_2) and non-brominated fluorocarbons (CF_3CHFCF_3, HFC-227ea and CF_3CH_2F, HFC-134a.

E. IMPORTANT FINDINGS AND CONCLUSIONS

- The use of Halon 1301 as a "baseline" for inhibitor mechanistic studies must be done with care since bromine's effect is not typical of catalytic suppressants in many respects. For CF_3Br, almost no effect of chemical saturation is observed compared to the “superagents”. Br only reduces radical concentrations to a significant extent in a narrow region of the flame. NaOH and $Fe(CO)_5$ reduce radical concentrations wherever they exceed equilibrium values.
- For chemical catalytic “superagents”, flame speed follows the peak H atom concentration and global activation energy for most agents. For halogen compounds (including HBr and CF3Br), H atom reduction occurs early in flame zone, not at the location of peak H concentration.
- For suppression effectiveness, selective depletion of H atoms early in the flame (at lower flame temperatures) has the greatest effect on burning velocity reduction.

- For catalytic inhibitors, ability to start the catalytic scavenging cycle early in the flame is critical for maximum effectiveness.
- Combining physical and chemical suppression is key to optimum suppression performance whether from a single agent or where two agents are combined.
- Experimental and modeling studies show that temperature reduction from physical suppression greatly enhances extinction effectiveness of "superagents".
- Favorable bond energy of key catalytic players is necessary (but not sufficient) for good suppression.
- Predictions of required concentrations for tin suggest that it is not a likely "superagent".
- For combined agents, the formation of stable fluorides limits the usefulness of combining fluorocarbons with a number of chemical agents. The choice of physical agents is likely to be limited to inert gases or liquids (e.g. water, if the chemical agent is a water soluble salt).

F. SIGNIFICANT HARDWARE DEVELOPMENTS (none)

G. SPECIAL COMMENTS

The chemistry of suppression has been a topic of intellectual curiosity and active research for a number of years. Through the efforts of the Next Generation Plan program, the conclusions and implications of several of these findings have been re-examined (taking advantage of advances in laboratory diagnostic capabilities and computation resources) and some re-interpreted in light of more recent data providing key details. Mechanistic studies have more clearly defined the suppression picture and documented what does not work and why. The NGP program has also made possible the examination of suppression mechanisms with the express intent of identifying alternative agents in a concentrated, methodical manner, involving scientists from a number of backgrounds including physics and chemistry, mechanical and fire protection engineering, and environmental and health sciences.

H. IMPLICATIONS FOR FUTURE RESEARCH

Superagents identified to date have very differing physical properties. Evaluation of their effectiveness presents problems when attempting an absolute effectiveness determination. There are limited options to achieve the sought after high efficiency suppression levels. The best choice will be a compromise between the physical properties and the specific applications that must be protected. Thus an evaluation on a case by case basis must be carried out.

II. ARTICLES PUBLISHED

Papers supported in whole or in part by this project

1. "Determination of the Strain in Counterflow Diffusion Flames From Flow Conditions", E.M. Fisher, B.A. Williams, and J.W. Fleming, Proceedings of the Eastern States Section: The Combustion Institute, pp. 191-194, 1997.
2. "Suppression Mechanisms of Alkali Metal Compounds", B.A. Williams and J.W. Fleming, Proceedings of the 1999 Halon Options Technical Working Conference, pp. 157-169, 1999.
3. "Flow Field Considerations for Counter Flow Burners", M.P. Davis, J.W. Fleming, B.A.

Williams, and H.D. Ladouceur, Proceedings of the Fall Technical Meeting of the Eastern States Section of the Combustion Institute, pp. 200-203, 1999.

4. “Chemical Fire Suppressants: How Can We Replace Halon?”, (invited presentation) Proceedings of the Fall Technical Meeting of the Eastern States Section of the Combustion Institute, pp. 16-23, 1999.
5. “Inhibition of Premixed Methane-Air Flames by Water Mist”, S.P. Fuss, D.J. Dye, B.A. Williams, and J.W. Fleming, Proceedings of the Fall Technical Meeting of the Eastern States Section of the Combustion Institute, pp. 105-108, 1999.
6. "Equivalence of the Ranking of Inhibitor Effectiveness for Combustion of Hydrocarbon Fuels", V.Babushok, W.Tsang, W.Grosshandler, Proceedings of the Fall Technical Meeting of the Eastern States Section of the Combustion Institute, pp. 180-183, 1999.
7. "Controlling the Self-Ignition Behavior of Silane", Tsang, W., Babushok, V., Proceedings of the Fall Technical Meeting of the Eastern States Section of the Combustion Institute, pp. 229-232, 1999.
8. "Influence of Phosphorus-Containing Fire Suppressants on Flame Propagation", Babushok, V., Tsang, W., Proceedings of the Third International Conference on Fire Research and Engineering, pp. 257-267, 1999.
9. “Inhibition of Premixed Methane-Air Flames by Submicron Water Mists”, S.P. Fuss, D.J. Dye, B.A. Williams, and J.W. Fleming, Proceedings of the 2000 Halon Options Technical Working Conference, pp. 242-250, 2000.
10. “Inhibitor Rankings for Hydrocarbon Combustion", V.Babushok and W.Tsang, *Combust. Flame*. 123(4), 488-506, 2000.
11. "Reduction in Burning Velocity of Premixed Methane-Air Flames by Submicron Water Mist”, S.P. Fuss, D.J. Dye, B.A. Williams, and J.W. Fleming, 28th International Symposium on Combustion, Abstracts of Work-in-Progress Posters, Poster No. WIP 1-J13, p. 13, 2000.
12. "Is CF_3Br Representative of Efficient Fire Suppressants?", B.A. Williams and J.W. Fleming, Proceedings of the 2nd Joint Meeting of the US Sections of the Combustion Institute, (CD) 2001.
13. “Influence of Bond Energies on Catalytic Flame Inhibition: Implications for the Search for New Fire Suppressants”, Bradley A. Williams and James W. Fleming, NRL Memorandum Report, 2003.

III. DETAILED PROJECT DESCRIPTION

III A. Approach and Techniques

Compounds or families of compounds were selected from lists of suppressants compiled in other NGP efforts, the scientific literature, and by mechanistic insight gained as the project progressed. Compounds were selected that demonstrated essentially physical suppression, compounds that were characterized as efficient chemical suppressants, and compounds that combined both mechanisms of suppression. Compounds or combinations of compounds were selected which could give guidance on the development of suppression systems, and demonstrate and characterize the combined effects of physical and chemical inhibition.

Both counterflow non-premixed flames and premixed Bunsen flames were considered. To simulate the typical mode of application, compounds were added to the air side of non-premixed counterflow flames. For the counterflow flames, the amount of additive to cause extinction was determined as a function of the extinction strain rate, maximum velocity gradient at extinction on the air side of the flame. For premixed flames, the effect of the additive concentration on the burning velocity was used to measure suppression effectiveness.

The additive effect on various aspects of the flame structure including flame species profiles and temperature as a function of additive concentration and flame strain rate were also examined.

Numerical simulations of inhibited and extinguishing flames using the latest computer codes were carried out. Kinetic rates and thermochemical data needed by the flame codes were assembled where available or developed where needed.

A major goal of the project was to determine whether the mechanisms of flame extinction by the addition of various agents were similar to or distinct from those exhibited by Halon 1301. It was intended that this insight would guide the search for and/or help to identify additional potential superagents.

The Combustion Dynamics Section of the Navy Technology Center for Safety and Survivability at the Naval Research Laboratory (NRL) carried out this project in collaboration with Drs. Wing Tsang and Valeri Babushok at NIST. Results specific for the NRL effort are detailed below. In the first year of the project, NRL collaborated with the Ignition and Combustion Branch, Propulsion and Flight Division, Weapons and Materials Research Directorate, of the Army Research Laboratory (ARL/WMRD). Details and findings of the Army 2a mechanism effort are documented in a separate report. Drs. Wing Tsang and Valeri Babushok and colleagues at NIST also collaborated on several other NGP projects closely related to the mechanism investigation. Those results are reported under the specific NGP projects.

III B. Suitability of CF_3Br as a Mechanism Benchmark for Fire Suppression

To assess whether CF_3Br is "typical" of efficient fire suppressants in general, premixed flames containing representative inhibitors of various types, including inert gases, fluorocarbons, and catalytic scavengers of flame radicals were modeled. Representatives from various suppression groups were selected. Those groups included: physical suppressants (such as nitrogen, argon, CF_4, and water) that do not participate in flame chemistry to a significant extent and inhibit combustion by adding heat capacity and diluting the reactants; chemical suppressants that participate in the flame chemistry and can be subdivided into catalytic suppressants (including bromine, iodine, and various metallic elements) which reduce concentrations of flame radicals through a regenerative cycle (one molecule of suppressant can recombine several radicals) and noncatalytic suppressants (e. g. fluorocarbons) that also reduce concentrations of flame radicals by scavenging flame radicals, at least in certain regions of the flame, but do not exhibit a catalytic cycle and are generally less effective. CF_3Br is primarily a catalytic suppressant [Sheinson, 1989], due to an H + H recombination cycle involving the bromine atom, although the CF_3 moiety adds some noncatalytic suppression as well.

The effectiveness of an inhibitor may be placed on a quantitative basis by considering an "inhibition parameter" Φ first proposed by Rosser *et al.* [Rosser, 1958] and modified by Noto *et al.* [Noto, 1998]:

$$\Phi = \ln(U_0/U_i) \text{ x } (X_{O2}/X_i) \qquad (1)$$

where U_0 and U_i are the burning velocities of the uninhibited and inhibited flames, respectively, and X_{O2} and X_i are the reactant mole fractions of oxygen and inhibitor. In [Noto, 1998] the burning velocity of a given fuel/air mixture was shown to exhibit an exponential dependence on the inhibitor concentration. This exponential dependence, by which the inhibition parameter was defined, was shown to hold for the inert agents N_2 and CF_4, several hydrofluorocarbons, and CF_3Br. Since catalytic scavengers intrinsically exhibit saturation effects (the concentrations of flame radicals, which typically exist in superequilibrium, cannot be reduced below the thermal equilibrium values at the local flame temperature) the existence of a similarity relation describing inhibition by CF_3Br as well as noncatalytic agents is somewhat unexpected. Saso *et al.* [Saso, 1999] modeled the combined effect of CF_3Br/inert inhibitors and found synergism (the two agents in combination had a greater inhibiting effect than the additive effect of the agents in isolation). The behavior was attributed to a temperature effect on the inhibition effectiveness of CF_3Br, rather than a saturation phenomenon. Over a range of adiabatic flame temperatures, Saso *et al.* found CF_3Br to have virtually identical inhibition parameters at concentrations of 0.5% and 1% in methane/oxygen/inert mixtures, once again suggesting the absence of significant saturation effects.

III C. Suppressant Effect On Burning Velocities and Species Profiles in Inhibited Premixed Flames

In the calculations described below, the PREMIX code [Kee, 1985] was used to compute burning velocities and flame structures of atmospheric pressure flames. An 85 cm domain was used in the calculations. Comparison with thermal equilibrium calculations showed that at the final grid point, temperatures were generally within 5K and radical concentrations within a few percent of their equilibrium values. Flames were stoichiometric, atmospheric pressure methane/oxygen, with various inhibitors added as indicated below.

For the hydrocarbon chemistry, GRIMech2.11 was used as the kinetic mechanism. Fluorocarbon chemistry was based on mechanism refinement previously performed in our laboratory [L'Esperance, 2000; Williams, 2000]. Bromine chemistry used for CF_3Br was that developed by Noto et al. [Noto, 1998]. The kinetic mechanism for sodium was based on that of [Zamansky, 1999], while that for $Fe(CO)_5$ was described by [Rumminger, 2000].

In Figures 1-3, changes in burning velocity, adiabatic flame temperature, radical superequilibrium, as well as the inhibition parameter Φ as defined by [Noto, 1998] are plotted as a function of inhibitor concentration. Note that a constant value of Φ indicates that the exponential dependence of flame speed on inhibitor concentration is well observed. The three plots compare the changes in the flame structure caused by CF_3Br with that of nitrogen (an inert agent) and sodium hydroxide (a catalytic agent). Nitrogen has a modest inhibition parameter (approximately 0.5) nearly independent of its concentration. The adiabatic flame temperature must be lowered by nearly 300K for the burning velocity to be reduced by 50%. While the peak concentrations of the flame radicals H, O, and OH decrease as the flame is inhibited, the peak concentrations normalized by the equilibrium values at the adiabatic flame temperature increase. This phenomenon provides a basis for the synergy observed between a catalytic and a physical agent, since a flame inhibited by a physical agent has a greater radical superequilibrium which the catalytic agent can exploit.

In the flame inhibited by NaOH, by contrast, the flame speed is reduced by 50% with virtually no change in the adiabatic temperature. The radical superequilibrium is drastically reduced as the inhibitor is added, eventually reaching unity for all primary flame radicals for a sufficiently large inhibitor concentration (meaning that the radical concentrations never overshoot their equilibrium values). Most notably, the inhibition parameter is not constant as a function of inhibitor concentration, but varies by more than a factor of three over the range of sodium concentrations considered here. The similarity relationship identified by Noto *et al*. does not hold for sodium.

For inhibition by CF_3Br, the flame speed is again reduced with little change in the adiabatic temperature (about 40K for the range of concentrations shown in the Figure 3). The degree of radical superequilibrium is reduced with increasing agent concentration, though not as dramatically as for sodium. By both of these measures, CF_3Br shows behavior typical of catalytic agents. The inhibition parameter, unlike for sodium, is nearly constant as a function of inhibitor concentration (except for the initial data point at an inhibitor concentration of 0.1% which has a high uncertainty due to the small differences in flame speeds). This nearly constant inhibition parameter was found by [Noto, 1998] although the modifications to the fluorocarbon kinetics yield somewhat higher inhibition parameters, in excellent agreement with the experimental value of 14.0 [Saso, 1999].

This raises the question of why the exponential relationship between burning velocity and inhibitor concentration is observed for CF_3Br but not for other chemical inhibitors. The present results support the conclusion of Saso *et al*. that saturation is a minor effect in the suppression effectiveness of CF_3Br/inert mixtures. One point is that for inhibition by CF_3Br, the H atom superequilibrium is only reduced by some 30% for a 50% reduction in flame speed, whereas for NaOH the H atom superequilibrium is reduced by nearly 80% for the same reduction in flame speed. Thus saturation is not as pronounced for CF_3Br in part because the peak radical concentrations are still far out of equilibrium even when the burning velocity has been substantially reduced.

The other important point for CF_3Br is that the bromine catalytic cycle involves the sequence of reactions [Westbrook 1980]

$$Br + Br + M \Rightarrow Br_2 + M \quad \text{(i)}$$

$$H + Br_2 \Rightarrow HBr + Br \quad \text{(ii)}$$

as an important pathway in regeneration of HBr, since the direct reaction

$$H + Br + M \Rightarrow HBr + M \quad \text{(iii)}$$

has rather slow kinetics. This has two consequences: the increasing importance of Reaction (i) (since it has a second order dependence on the inhibitor concentration) compensates for the saturation effect as the inhibitor concentration is increased. Also, a much higher concentration of bromine is required for this reaction to be significant. Compared to sodium and iron, whose suppression kinetics are not thought to depend significantly on any second order pathways, bromine is a relatively inefficient scavenger.

III D. Combined Effects of Mixtures of Agents

Since various studies have described synergism of combinations of CF_3Br and inert agents, it is worth exploring to what extent the observations carry over to other combinations of agents. Furthermore, it is worth exploring whether there is any advantage to combining different chemical scavengers which act independently (i. e. recombine different flame radicals).

To this end, inhibition by iron was modeled in combination with both nitrogen and sodium. For this modeling, iron was considered to participate in a three step mechanism involving only O + O recombination. This pathway was identified by [Rumminger, 2000] but is usually secondary in importance to an H + H recombination pathway. Using this simplified model, sodium and iron do not directly compete for the same flame radicals, since sodium primarily undergoes an H + OH recombination cycle. This model is *not* intended as an accurate description of iron's combustion chemistry but to investigate the combined effect of scavengers that operate through different pathways.

In Table 3, the effects of iron and sodium both separately and in combination, are listed. The effectiveness of the inhibitors when combined are described by their "differential inhibition parameters.” The differential inhibition parameter of substance A is determined by comparing the burning velocity of a mixture inhibited by A and B in combination, to that of the mixture inhibited by B alone. As seen in Table 3, the differential inhibition parameters of iron and sodium in combination are much less than those of the two elements taken separately. Even though the two elements do not directly compete for the same flame radicals, the rapid exchange between H, O, and OH means that the two suppressants reduce each other's effectiveness.

Iron, in combination with nitrogen, does exhibit synergy. Figure 4 shows the burning velocity, flame temperature, and differential inhibition parameter of iron (using the O + O recombination mechanism) as a function of nitrogen addition to a methane/air mixture. The differential inhibition parameter of 500 ppm FeO_2 increases by some 23% as the flame temperature is lowered by nitrogen addition from 2230K to 2010K. These results may be compared to those of Saso *et al*. [Saso, 1999], who found that the inhibition parameter of CF_3Br increased by some 45% (at both 0.5% and 1.0% mole fractions of agent) over the same range of final flame temperatures. While the findings of synergism agree qualitatively, the final flame temperature influences the inhibition parameter of CF_3Br twice as much as that of the O + O recombination cycle of iron. Therefore while synergism in catalytic/inert mixtures may be a general characteristic, its magnitude can vary considerably depending on the kinetics of the catalytic component.

III E. Correlation of Burning Velocity, Final Flame Temperature, and Flame Radical Concentrations

According to laminar flame theory, the burning velocity of a premixed flame is proportional to the square root of the overall reaction rate. In modeling the burning velocity of a large number of inhibited flames, the burning velocity correlates in almost all cases with the product of the peak H atom mole fraction and a global activation energy:

$$S_L^2 = A^2 X_H \exp(-E_a/kT_f) \tag{2}$$

where S_L is the laminar burning velocity, X_H the peak mole fraction of atomic hydrogen, and T_f the final flame temperature. The fitted parameters A and Ea, obtained by considering the flame inhibited by nitrogen, are A=7940 cm/s, E_a=24.7 kcal/mol. The same empirical correlation holds for inhibition by other inert gases, by iron and sodium, by nitrogen and iron in combination (Figure 4), and by artificially increasing the H + OH recombination rate. For the catalytic agents, which do not cause appreciable changes in the final flame temperature, the flame speed correlates with the peak mole fraction of atomic hydrogen, but not with that of atomic oxygen or OH radicals.

Padley and Sugden [Padley, 1958] observed in studies of $H_2/O_2/N_2$ flames that the burning velocity correlated with the partial pressure of atomic hydrogen in the reaction zone. More recently, this correlation has been observed to hold also for hydrogen flames inhibited by CF_3Br [Kim, 2001]. Figure 4 plots the peak H atom concentration against burning velocity for a variety of inhibited methane/air flames. For methane flames inhibited by N_2, CF_4, and CF_3Br, there is a nearly identical linear relationship between the peak H atom mole fraction and burning velocity, as with the hydrogen flames.

The observation that atomic hydrogen controls the burning velocity is not unexpected, due to the high diffusivity and reactivity of this species. Nevertheless, some noteworthy conclusions can be made: 1) this correlation can quantitatively describe the effect of a wide variety of inhibitors, both individually and in combination; 2) catalytic agents reduce the flame speed by reducing the atomic hydrogen concentration, whether or not the scavenging cycle directly involves H atom recombination. The partial equilibrium between H, O, and OH is not disrupted in most inhibited flames.

Table 2 compares the burning velocities estimated using Equation (2) to the calculated values for a variety of flame inhibitors. In almost all cases, the reduction in burning velocity relative to the uninhibited flame, predicted by Equation (2) is within 10% of the actual value using the full kinetics. This relationship between burning velocity, final flame temperature, and peak H atom mole fraction holds for many agents (both catalytic and inert) and also when one artificially increases the H + OH recombination rate. At the same time, there are a few notable exceptions: the fluorocarbons CHF_3 and C_3HF_7 are much better inhibitors (by nearly a factor of two) than Equation (2) would predict. So are both CF_3Br and HBr. Flame structure modeling indicates that the breakdown of this relationship involving the peak H atom concentration is a consequence of these agents reducing the H atom concentration mostly in the early part of the flame, as demonstrated below.

III F. Changes in Flame Structure Due to Different Agents

The explanation for why the correlation between flame speed, H atom concentration, and temperature does not hold for either fluorocarbons or bromine containing compounds can be gained from examination of these compounds' effects on flame structure. In Figure 5 the mole fraction of atomic hydrogen is plotted against the local temperature for flames inhibited by the inert agent N_2, the catalytic agent $Fe(CO)_5$, the noncatalytic fluorocarbon CF_3CHFCF_3, and CF_3Br. All the inhibited flames have burning velocities approximately 50% that of the uninhibited flame, whose structure is also plotted for comparison. For all the flames considered here, temperature overshoot does not occur; the temperature monotonically increases with position passing from reactants to products.

The way in which the relationship between H atom mole fraction and local temperature is altered is characteristic of each type of agent. Other agents modeled (not shown on the plot for clarity) produce H atom profiles which closely resemble each other within the same class: CF_4 and N_2, NaOH and $Fe(CO)_5$, CH_2FCF_3 and CF_3CHFCF_3. The physical agents reduce the final flame temperature, but the H atom mole fraction at a given isotherm (above approximately 1300K) is changed very little from its value in the uninhibited flame. Both iron and sodium reduce the H atom mole fraction by a relatively constant factor throughout the reaction zone, in other words the inhibition occurs throughout the flame. The fluorocarbons, on the other hand, reduce the H atom mole fraction early in the flame (in the region below about 1200K) but have relatively little impact on the peak concentration. The same situation occurs for CF_3Br; in this respect CF_3Br bears more resemblance to non-brominated fluorocarbons than it does to other catalytic agents such as iron and sodium.

The depletion of radical species early in the flame has a marked influence on the flame speed. It is for this reason that fluorocarbons and bromine compounds are better inhibitors than the changes in temperature and peak H atom concentrations would predict. This observation implies that agents which deplete radicals in high temperature regions but not early in the flame are likely to be less effective inhibitors than would otherwise be expected. This may be the case, for instance, for condensed-phase agents which must undergo a vaporization process before inhibition chemistry can begin.

III G. Influence of Bond Energies on Suppression Cycles

For a substance to catalytically scavenge flame radicals, there must exist some species X derived from the inhibitor which can bond to H, O, or OH. The species XR, where R is one of the flame radicals, must react with another flame radical R' to form X and RR', where RR' is usually a stable molecule such as H_2, H_2O, or O_2. Possible scavenging reactions include

$XH + H => X + H_2$ (R1)
$XH + OH => X + H_2O$ (R2)
$XOH + H => X + H_2O$ (R3
$XO + O => X + O_2$ (R4)

For an efficient scavenging cycle to exist, the bond energy between the scavenging atom or radical X and a flame radical R must satisfy certain conditions. If it is too high, the scavenging reaction (R1)-(R4) will be endothermic. This is the case for fluorine, which binds irreversibly to hydrogen and thus cannot sustain a catalytic cycle. On the other hand, if the bond is too weak, equilibrium between XR and X + R will be so far toward dissociation that there will be insufficient XR to participate in the scavenging reactions. Stated another way, the rates of the reverse reactions should be small compared to those of the forward reactions, since any catalytic recombination cycle will become a catalytic chain branching cycle if it runs backwards.

These considerations indicate that there will be a limited range of bond energies for which an efficient scavenging cycle can exist. Putting these qualitative arguments on a quantitative basis by computational investigation of the effect of hypothetical changes in bond energies on suppression efficiencies allows the determination of the bond energies compatible with efficient suppression. Suppression depends on kinetic as well as thermodynamic factors, so appropriate bond energies by themselves do not guarantee good suppression properties. The elements chosen here as examples, however, are known to have good suppression properties, so they possess kinetics favorable to scavenging.

Bromine was used as the example element for Reactions (R1) and (R2), sodium for (R3), and iron for (R4). All of these elements have several bond energies which may be hypothetically relevant to combustion. In order to simplify the situation so that sensitivity to bond energy can be determined in a relatively straightforward way, it was assumed that only one catalytic cycle involving one type of bond existed for each element.

For each set of calculations, the thermodynamic functions for the species XR were not altered, but heat of formation of the species X at 298K was varied, while keeping the heat capacity and entropy unchanged. This has the effect of changing the dissociation energy of X-R. In the kinetic mechanisms, the chemical reactions for the scavenging cycle were written in the exothermic direction, and the Arrhenius parameters of the forward reaction were unchanged. All reactions are assumed to be reversible, however, so changing the heat of formation alters the activation energy of the reverse reaction, even without any explicit changes to the kinetic parameters.

III G 1. Bromine: H + H and H + OH Recombination

For this series of calculations HBr was chosen as the bromine containing reactant. The kinetic mechanism was chosen to model the effect of a single catalytic mechanism, with Br and HBr as the only bromine species. Two sets of calculations were performed, the difference being whether HBr was assumed to react with H or with OH. Figure 7 shows the predicted flame speed of a stoichiometric methane/air mixture inhibited by an 0.5% mole fraction of HBr. The catalytic cycle is most efficient for H-Br bond energies between 65 and 90 kcal/mole.

The accepted value of the H-Br bond energy lies near the upper limit of the range that permits an efficient catalytic cycle (Figure 7). The bond energy of H-I is near the lower limit of the optimal range, while the H-Cl bond is too strong for good suppression. The bond energy of H-F (135 kcal/mole) is so high that it is completely inert in this environment. Although kinetics of the analogous reactions are somewhat different for the other halogens, the bond energy factor by itself leads to the correct prediction that iodine has a suppression effect nearly equal that of bromine, while chlorine has a much smaller effect.

The peak efficiency of the cycle assuming an H + OH net recombination is lower than for the H + H cycle, in accord with analysis [Casias, 1998] of detailed modeling of the pathways of CF_3Br, in which the reaction of HBr with H is found to be more important than the reaction with OH. It is noteworthy that at the value of the bond energy of H-Cl, the H + OH cycle is more efficient than the H + H cycle, due to the higher dissociation energy of water compared to molecular hydrogen. This indicates that the (small) catalytic effect of HCl is primarily due to its reaction with OH rather than with H.

III G 2. Sodium: OH + H Recombination

The effect of hypothetical variation of the Na-OH bond energy is illustrated in Figure 8. There is a more pronounced falloff in suppression efficiency with bond energy than for either of the bromine scavenging cycles. It is seen that the Na-OH bond energy is close to the optimal value for good suppression, as are the bond energies for all the other alkali metals except lithium. Experimental studies have found that potassium is a considerably more efficient suppressant than sodium [Babushok, 2000]. In view of the similarity of the thermodynamic properties, this difference may be due to differences in kinetic rates between the two elements, particularly for the recombination step $X + OH + M \rightarrow XOH + M$.

III G 3. Iron: O + O Recombination

The three step O + O catalytic cycle modeled for iron has two relevant bond energies, Fe-O and OFe-O, which differ by about 3 kcal/mole. The bond energies were varied in the calculation by keeping the standard state enthalpy of FeO fixed, while varying those of Fe and FeO_2 in opposite directions from their "normal" values. For FeO_2, the "normal" standard state enthalpy used was not the actual value, but was chosen such that the bond energy of OFe-O was equal to that of Fe-O, 99 kcal/mole. Results of the calculations are shown in Figure 9. The accepted bond energies of both Fe-O (99 kcal/mol) and OFe-O (96 kcal/mol) are close to the optimal value for efficiency of the catalytic cycle.

III G 4. Effect of Bond Energies on Suppression Cycles: Conclusions

For efficient scavenging cycles, it appears that the bond energy between a catalytic scavenger and a flame radical must lie in the range of 70-100 kcal/mol, the optimal value varying somewhat for different net recombination reactions. This range of values is consistent with the expectation that the bond must be strong enough to be thermodynamically stable at flame temperatures, but not so strong as to prevent regeneration of the active scavenging radical.

IV. RECOMMENDATIONS FOR ADDITIONAL RESEARCH

A great number of compounds (through their individual metal constituents) were considered and/or tested in this and related mechanism projects. It is clear that after eliminating those elements that clearly will not work, there are only a limited number of compounds that are capable of providing the ultra-high efficiency sought after and still satisfy the environmental and health safety concerns. These compounds have different physical properties and must be evaluated on a case by case basis for specific applications.

V. CONCLUSIONS

CF_3Br is an efficient fire suppression agent that can be used to assess the overall effectiveness of potential replacement agents. Using the effectiveness of CF_3Br as a extinguishment benchmark has merit. However, as pointed out in this project, the suppression mechanism of CF_3Br is not typical of efficient fire suppressants, and certainly not similar to the ultra-high efficient agents. The anomalous suppression behavior of CF_3Br is specifically related to the flame kinetics of bromine. Demanding a replacement agent display the same suppression mechanism as CF_3Br essentially requires that the replacement agent also contain bromine. However, the role of bromine in the destruction of stratospheric ozone is the reason replacements are needed. Providing the bromine on a compound that will not survive intact as it travels through the troposphere (tropodegradable) is one approach currently pursued by the NGP.

In order to achieve ultra-high suppression efficiency, a replacement agent (or a species provided by the agent) must participate in the catalytic removal of the key flame propagation radicals: H, O, or OH. There are several species whose chemistry permits this behavior including the alkali metals, iron, phosphorus, and manganese. Of these so-called superagents, iron has been shown to be the most efficient at flame speed inhibition. Three principles control the efficiency of catalytic superagents. First, a sufficiently large enough concentration of the catalytic species must be achievable at the flame condition (fundamental limitation due to thermodynamics and the system temperature and composition). Second, the catalyst can only take the flame radicals to their equilibrium concentration at that flame temperature. If the equilibrium concentrations of the flame radicals are still sufficient to maintain combustion, then in the absence of any other heat losses, extinguishment will never be achieved. The use of a thermal agent to lower the flame radical equilibrium concentration amount can be exploited. Extinction can be achieved by combining the chemical catalytic ultra-efficient agent and a thermal agent. However, the first principle mentioned above cannot be violated; a sufficient concentration of the catalytic species must exist at the lower flame temperature. The inability of iron compounds to efficiently achieve extinction in some non-premixed flames (e.g. cup burner flames) is due to this limitation. The third controlling principle deals with the reactivity of the catalytic specie. It must significantly react only with the H, O, and OH flame radicals and not with any other species in the flame. The reactivity of fluorine (introduced by fluorinated thermal agents) limits the practical use of HFC thermal agents and most catalytic agents. The optimum ultra-efficient agent thus achieves extinction through a balance of achievable flame concentration, sufficient catalytic activity, and sufficient flame temperature reduction. This balance is optimally achieved by CF_3Br and can be met with other systems. In the search for viable, ultra-efficient replacement agents, chemistry is definitely important but there are thermodynamic limitations that must be assessed on a case by case basis.

VI. ACKNOWLEDGEMENTS

Valeri Babushok (NIST) was a co-PI on this project and contributed to the mechanistic understanding of iron, manganese, phosphorus, and tin. Contributions of Paul Fuss (NRL/ASEE Postdoc) are acknowledged. This project was supported by the Department of Defense Next-Generation Fire Suppressant Technology Program, funded by the DoD Strategic Environmental Research and Development Program. Partial funding was received from the Office of Naval Research through the Naval Research Laboratory.

VII. REFERENCES

Babushok, V. and Tsang, W., (2000), Inhibitor rankings for alkane combustion ,*Combust. Flame* **123**:488-506.

Casias, C. R., and McKinnon, J. T., (1998), A Modeling Study of the Mechanisms of Flame Inhibition by CF_3Br Fire Suppressant Agent, *Proc. Combust. Inst.*. **27**:2731-2740.

Kee, R.J., Grcar, J.F., Smooke, M.D., and Miller, J.A., (1985), *PREMIX: A Fortran Program for Modeling Laminar One-Dimensional Premixed Flames*, Sandia Report SAND85-8240.

Kim, C. H., Kwon, O. C., and Faeth, G. M., (2001), Second Joint Meeting of the U. S. Sections of the Combustion Institute, paper #219.

L'Espérance, D., Williams, B. A., and Fleming, J. W., (1999), Intermediate Species Profiles in Low Pressure Premixed Flames Inhibited by Fluoromethanes, *Combust. Flame* **117**:709-731.

Noto, T., Babushok, V., Hamins, A., and Tsang W., (1998), Inhibition effectiveness of halogenated compounds, *Combust. Flame* **112**:147-160.

Padley, P. J. and Sugden, T. M., (1958), *Proc. Combust. Inst.* **7**:235-242.

Rosser, W. A.., Wise, H., and Miller, J., (1958), Mechanism of Combustion Inhibition by Compounds Containing Halogen, *Proc. Combust. Inst*. **7**:175-182.

Rumminger, M. D., and Linteris, G. T., (2000), Inhibition of Premixed Carbon Monoxide-Hydrogen-Oxygen-Nitrogen Flames by Iron Pentacarbonyl, *Combust. Flame* **120**:451–464.

Saso, Y., Ogawa, Y., Saito, N., and Wang, H., (1999), Binary CF_3Br- and CHF_3-inert flame suppressants: Effect of temperature on the flame inhibition effectiveness of CF_3Br and CHF_3, *Combust. Flame* **118**:489-499.

Sheinson, R. S., Penner-Hahn, J. E., and Indritz, D., (1989), The Physical and Chemical Action of Fire Suppressants, *Fire Safety J*. **15**:437-450.

Westbrook, C. K., (1980), *Combust. Sci. Technol*. **23**:191-202.

Williams, B. A., L' Espérance, D. M., and Fleming, J. W., (2000), Intermediate Species Profiles in Low Pressure Methane/Oxygen Flames Inhibited by 2-H Heptafluoropropane: Comparison of Experimental Data with Kinetic Modeling, *Combust. Flame* **120**:160-172.

Zamansky, V. M., Lissianski, V. V., Maly, P. M., Ho, L., Rusli, D., and Gardiner, Jr., W. C., (1999), Reactions of Sodium Species in the Promoted SNCR Process, *Combust. Flame* **117**:821-831.

VIII. LIST OF TABLES

IX. LIST OF FIGURES

Figure 1: Flame speed, final flame temperature, inhibition parameter (defined in [Noto, 1998]), and superequilibrium concentrations of flame radicals computed for atmospheric pressure stoichiometric methane/air mixtures inhibited by nitrogen.

Figure 2: Flame speed, final flame temperature, inhibition parameter (defined in [Noto, 1998]), and superequilibrium concentrations of flame radicals computed for atmospheric pressure stoichiometric methane/air mixtures inhibited by sodium hydroxide. To simulate the evaporation process, NaOH was added to the reactants as a dimmer and required to undergo an endothermic decomposition process before inhibition chemistry could occur.

Figure 3: Flame speed, final flame temperature, inhibition parameter (defined in [Noto, 1998]), and superequilibrium concentrations of flame radicals computed for atmospheric pressure stoichiometric methane/air mixtures inhibited by CF_3Br.

Figure 4: Flame speed, differential inhibition parameter (see text), and superequilibrium concentrations of atomic hydrogen computed for atmospheric pressure stoichiometric methane/air mixtures inhibited by nitrogen and FeO_2 in combination.

Figure 5: Mole fraction of atomic hydrogen as a function of local flame temperature for an uninhibited atmospheric pressure methane/air flame, and the same flame inhibited by the indicated suppression agents.

Figure 6. Relationship between burning velocity and peak concentration of atomic hydrogen for methane air flames inhibited by various compounds. The N_2 + Fe data is that presented in Figure 4, containing a FeO_2 as a reactant assumed to operate via an O + O inhibition cycle.

Figure 7. Calculated flame speed as a function of H-Br bond energy (see text) for premixed methane/air flames inhibited by 0.5% HBr using the H + H and H + OH scavenging cycles of Table 3. The accepted values for the bond energies of H-Br, H-Cl, and H-I are indicated by vertical lines.

Figure 8. Calculated flame speed as a function of Na-OH bond energy (see text) for premixed methane/air flames inhibited by 0.1% $(NaOH)_2$ using the H + OH scavenging cycle of Table 3. The accepted values of X-OH bond energies for the alkali metals are indicated by vertical lines.

Figure 9. Calculated flame speed as a function of Fe-O bond energy (see text) for premixed methane/air flames inhibited by 500 ppm FeO_2 using the three step O + O scavenging cycle of Table 3. The accepted values of the Fe-O and OFe-O bond energies are indicated by vertical lines.

Table 1

Inhibition by Two Chemical Agents in Combination

Flame: stoichiometric methane/air, atmospheric pressure

Agent	Flame Speed (cm/s)	Inhibition Parameter Φ [Eqn. (1)]
none	39.6	---
0.2% $(NaOH)_2$	17.0	40.1[a]
0.1% FeO_2	29.5	56.1
0.1% FeO2 + 0.2%$(NaOH)_2$	14.9	24.9(Fe), 32.4(Na)[b]

[a] per sodium atom

[b] differential effect of specified inhibitor relative to other inhibitor alone.

Table 2
Comparison of Calculated Flame Speeds to Values from Equation (2)

$S_{eqn} = A(X_{H,max}*\exp(-E_a/kT_{ad}))^{1/2}$ A=7940 cm/s E_a=24.7 kcal/mol

flame condition	$T_{adiabatic}$	$X_H$max	S_{premix}	S_{eqn}	$\Delta S_{premix}/\Delta S_{eqn}$[a]
CH_4/air (uninhibited)	2234	6.64e-3	39.8	39.8	---
+3.85% N_2	2187	5.96e-3	35.5	35.6	1.01
+9.09% N_2	2121	5.12e-3	30.2	30.2	1.00
+13.04% N_2	2065	4.45e-3	26.1	26.0	0.99
+16.67% N_2	2015	3.94e-3	22.6	22.7	1.01
+8.26% CF_4 (inert)	1968	3.50e-3	18.4	19.9	1.07
+500ppm FeO_2 (O+O cycle)	2220	2.52e-3	33.3	32.7	0.92
+0.5%HBr (H+H cycle)	2221	5.36e-3	30.3	35.2	2.08
+0.5%HBr (H+OH cycle)	2220	5.47e-3	33.3	35.5	1.52
+5.2%CHF_3 (phi=1.1)	2036	4.04e-3	16.3	23.7	1.46
+3%C_3HF_7 (phi=0.9)	2161	3.86e-3	17.8	27.7	1.81
+0.05% $(NaOH)_2$	2219	2.97e-3	28.0	26.2	0.87
+0.40%$(NaOH)_2$	2177	3.31e-4	9.4	8.3	0.97
increase H + OH + M rate:					
x10	2234	4.04e-3	32.0	31.1	0.90
x100	2234	1.35e-3	19.8	18.0	0.92
x1000	2234	3.64e-4	11.2	9.3	0.94

[a] $(39.8-S_{premix})/(39.8-S_{eqn})$

Table 3

Kinetic Mechanisms for Suppressants

	$k = AT^b\exp(-E_a/kT)$			
	A(cm^3,mol,s)	b	E_a(cal/mol)	Remark.
Mechanism for Na (H + OH cycle only-Figure 8)				
$(NaOH)_2$+M=NaOH+NaOH+M [a]	3.0E14	0.0	48000	
NaOH+H=Na+H_2O	1.0E13	0.0	1970	
Na+OH+M=NaOH+M [a]	1.8E21	-1.0	0	
Mechanism for Br (reactions in common for all cycles)				
H + Br + M = HBr + M [a]	1.92E21	-1.86	0	[b]
Br + CH_2O = HBr + HCO	1.02E13	0.0	1590	[c]
Br + HO_2 = HBr + O_2	8.43E12	0.0	1172	[c]
Br + HCO = HBr + CO	1.69E14	0.0	0	[d]
Addition for Br (H + H cycle-Figure 7):				
HBr + H = H_2 + Br	6.25E13	0.0	2405	[b]
Addition for Br (H + OH cycle-Figure 7):				
HBr +OH = H_2O+ Br	6.62E12	0.0	0	[e]
Mechanism for Fe (O + O cycle-Figure 9):				
Fe + O_2 + M = FeO_2 + M [a]	1.57E18	0.0	4050	[f]
FeO_2 + O = FeO + O_2	1.73E13	0.0	0	estimated
FeO + O =Fe + O_2	1.73E13	0.0	0	[g]

[a] Third body efficiencies: H_2:2 H_2O:6 CH_4:2 CO:1.5 CO_2:2 C_2H_6:3

[b] Baulch, D.L., Duxbury, J., Grant, S.J., and Montague, D.C., *J. Phys. Chem. Ref. Data* 10: Suppl (1981).

[c] Atkinson, R., Baulch, D.L., Cox, R.A., Hampson, R.F., Jr., Kerr, J.A., Rossi, M.J., and Troe, J. *J. Phys. Chem. Ref. Data* 26:521-1011 (1997).

[d] Poulet, G., Laverdet, G., and LeBras, G., *J. Chem. Phys*. 80:1922 (1984).

[e] DeMore, W.B., Sander, S.P., Golden, D.M., Hampson, R.F., Kurylo, M.J., Howard, C.J., Ravishankara, A.R., Kolb, C.E., and Molina, M.J., *Chemical kinetics and photochemical data for use in stratospheric modeling. Evaluation number 12*, JPL Publication 97-4: 1-266 (1997).

[f] Helmer, M. and Plane, J.M.C., *J. Chem. Soc. Faraday Trans*. 90:395-401 (1994).

[g] based on reverse reaction: Akhmadov, U.S., Zaslonko, I.S., and Smirnov, V.N., *Kinet. Catal.* 29:251 (1988).

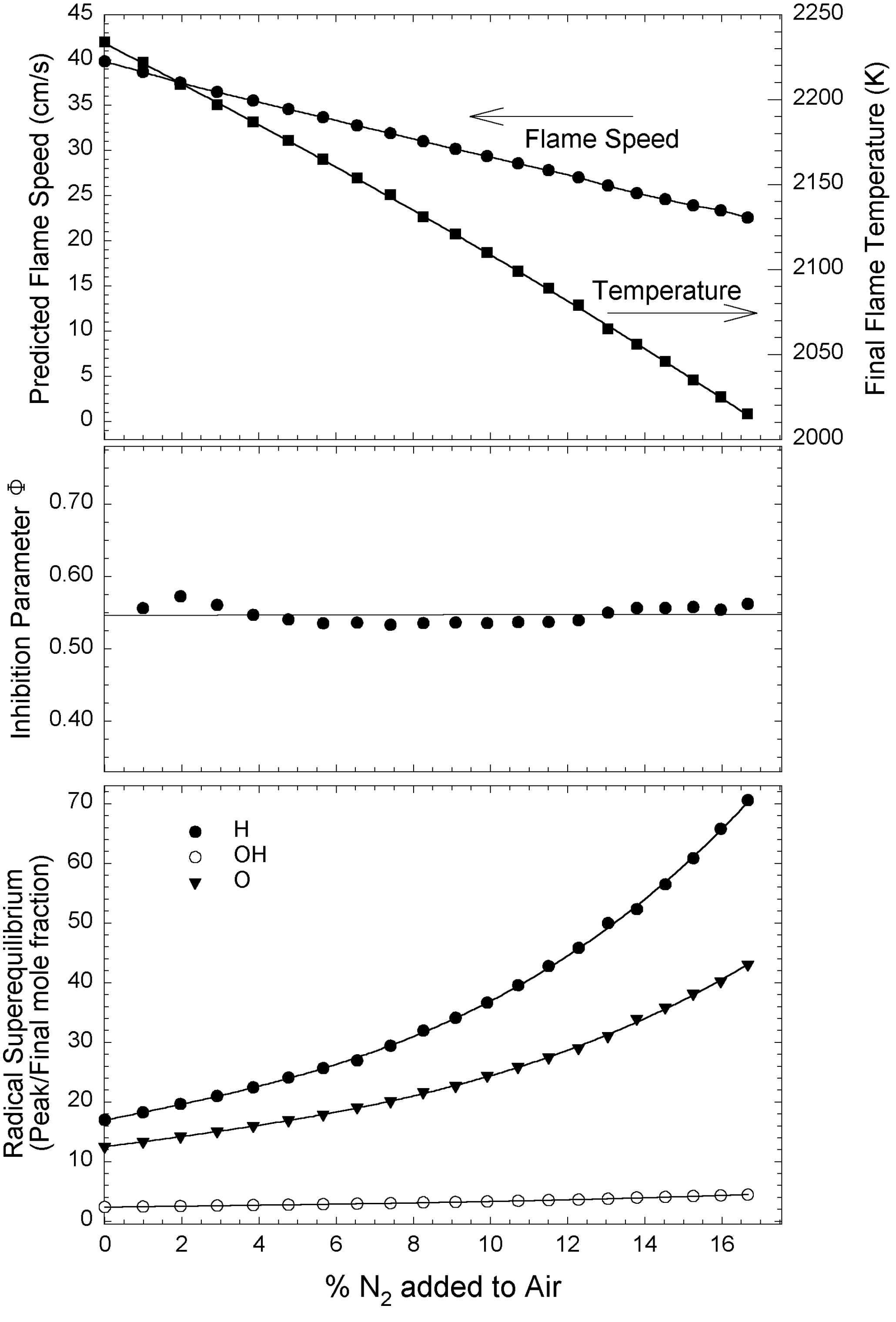

Figure 1: Flame speed, final flame temperature, inhibition parameter (defined in [Noto 1998]), and superequilibrium concentrations of flame radicals computed for atmospheric pressure stoichiometric methane/air mixtures inhibited by nitrogen.

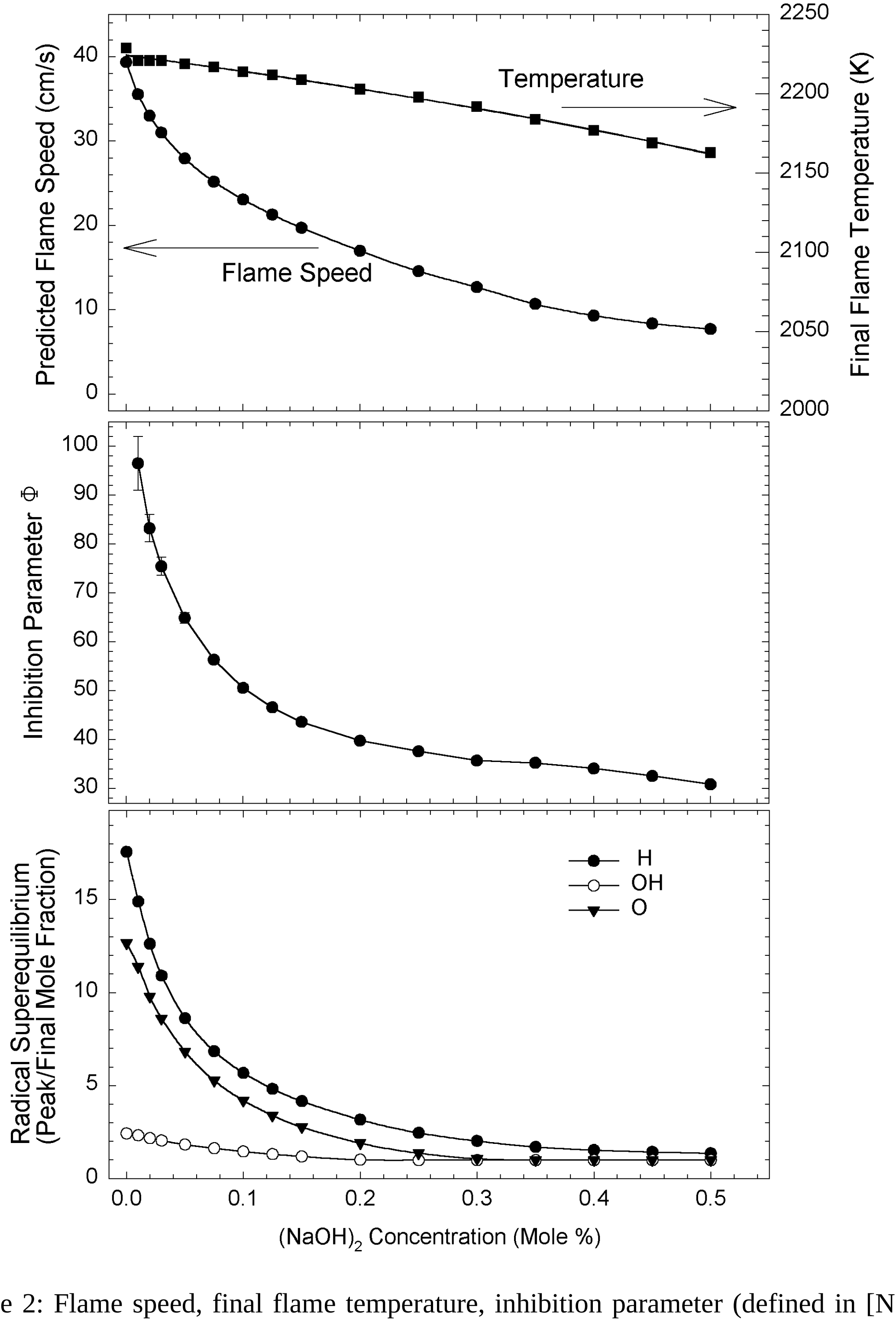

Figure 2: Flame speed, final flame temperature, inhibition parameter (defined in [Noto 1998]), and superequilibrium concentrations of flame radicals computed for atmospheric pressure stoichiometric methane/air mixtures inhibited by sodium hydroxide. To simulate the evaporation process, NaOH was added to the reactants as a dimmer and required to undergo an endothermic decomposition process before inhibition chemistry could occur.

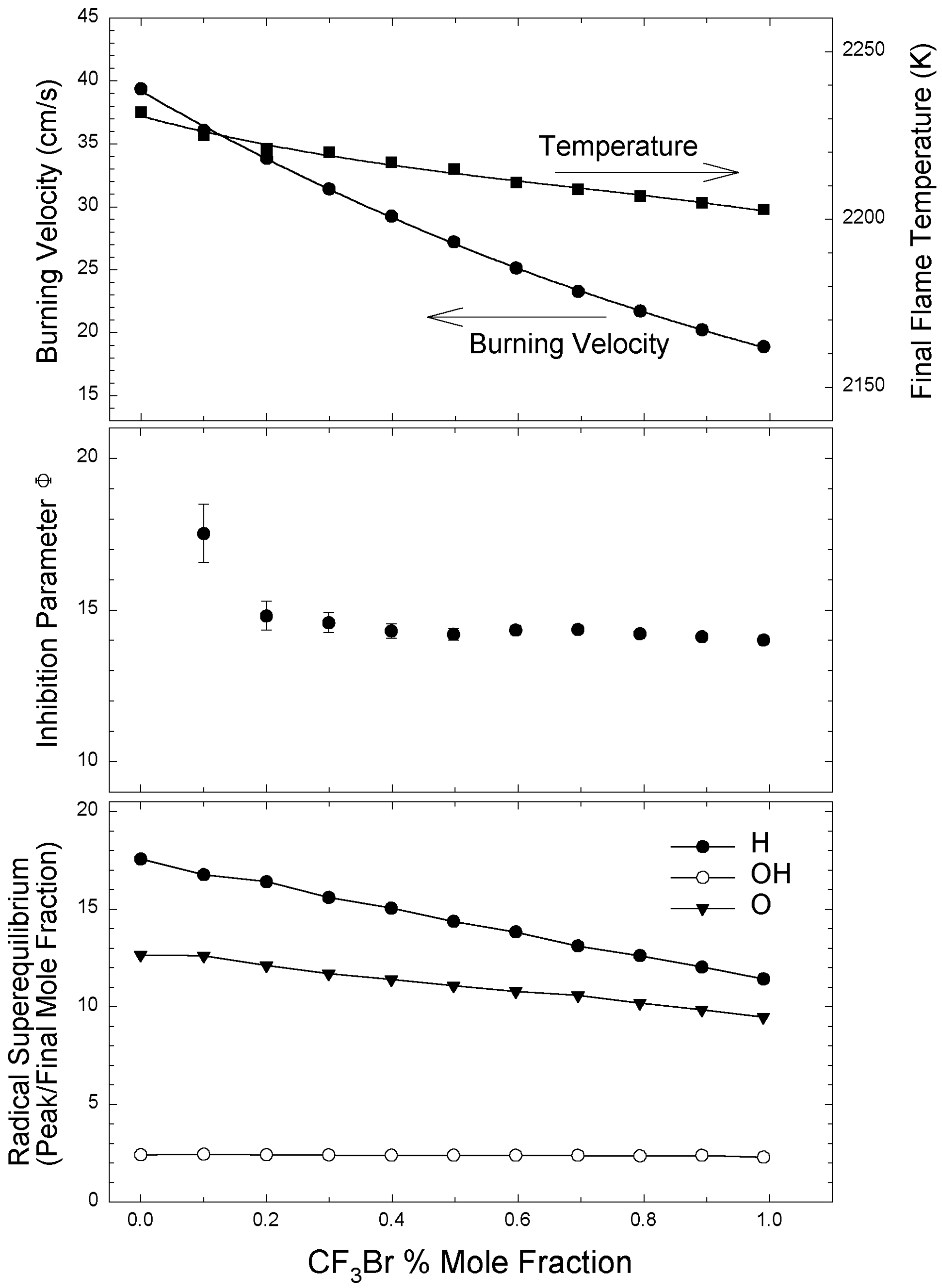

Figure 3: Flame speed, final flame temperature, inhibition parameter (defined in [Noto 1998]), and superequilibrium concentrations of flame radicals computed for atmospheric pressure stoichiometric methane/air mixtures inhibited by CF_3Br.

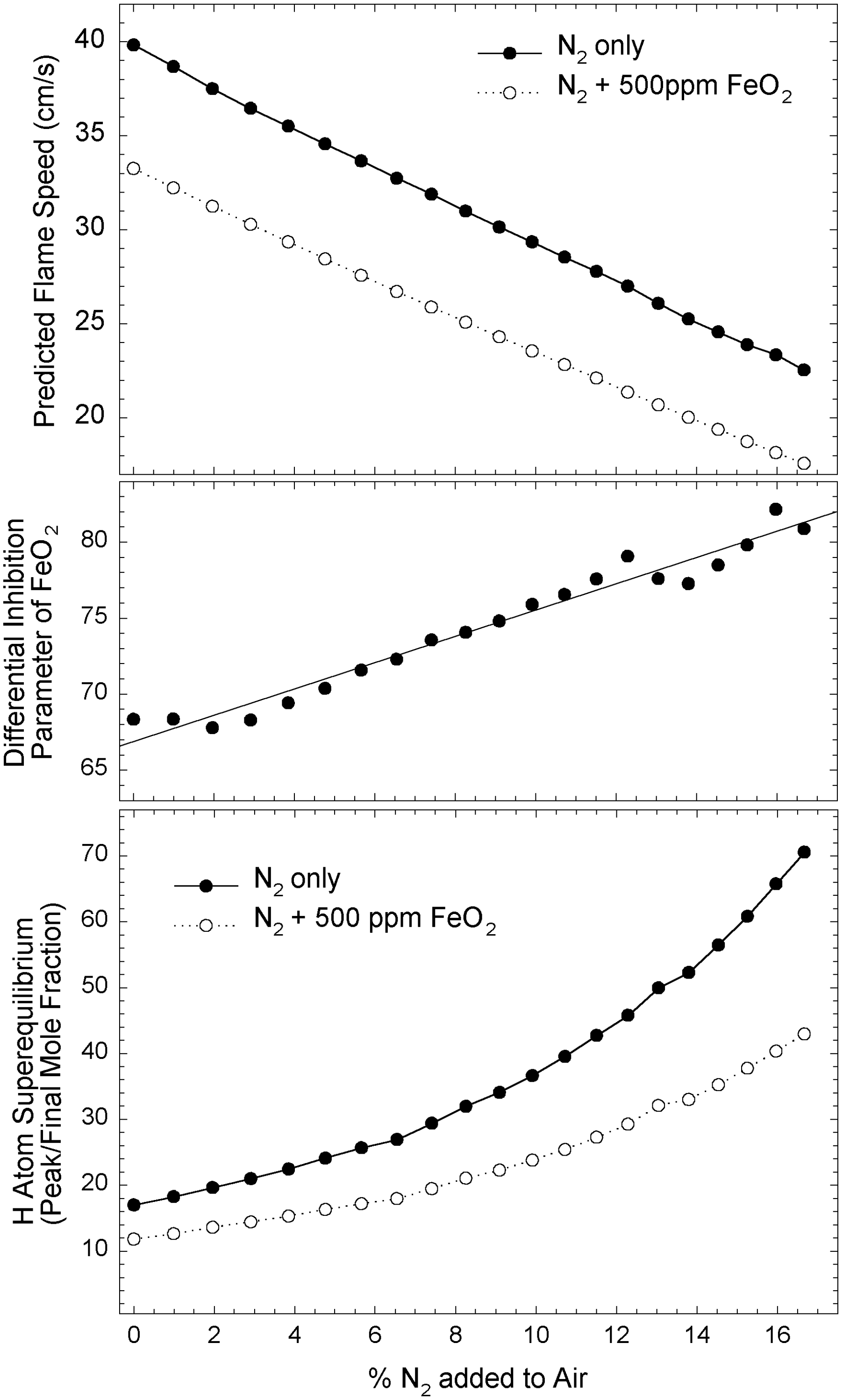

Figure 4: Flame speed, differential inhibition parameter (see text), and superequilibrium concentrations of atomic hydrogen computed for atmospheric pressure stoichiometric methane/air mixtures inhibited by nitrogen and FeO_2 in combination.

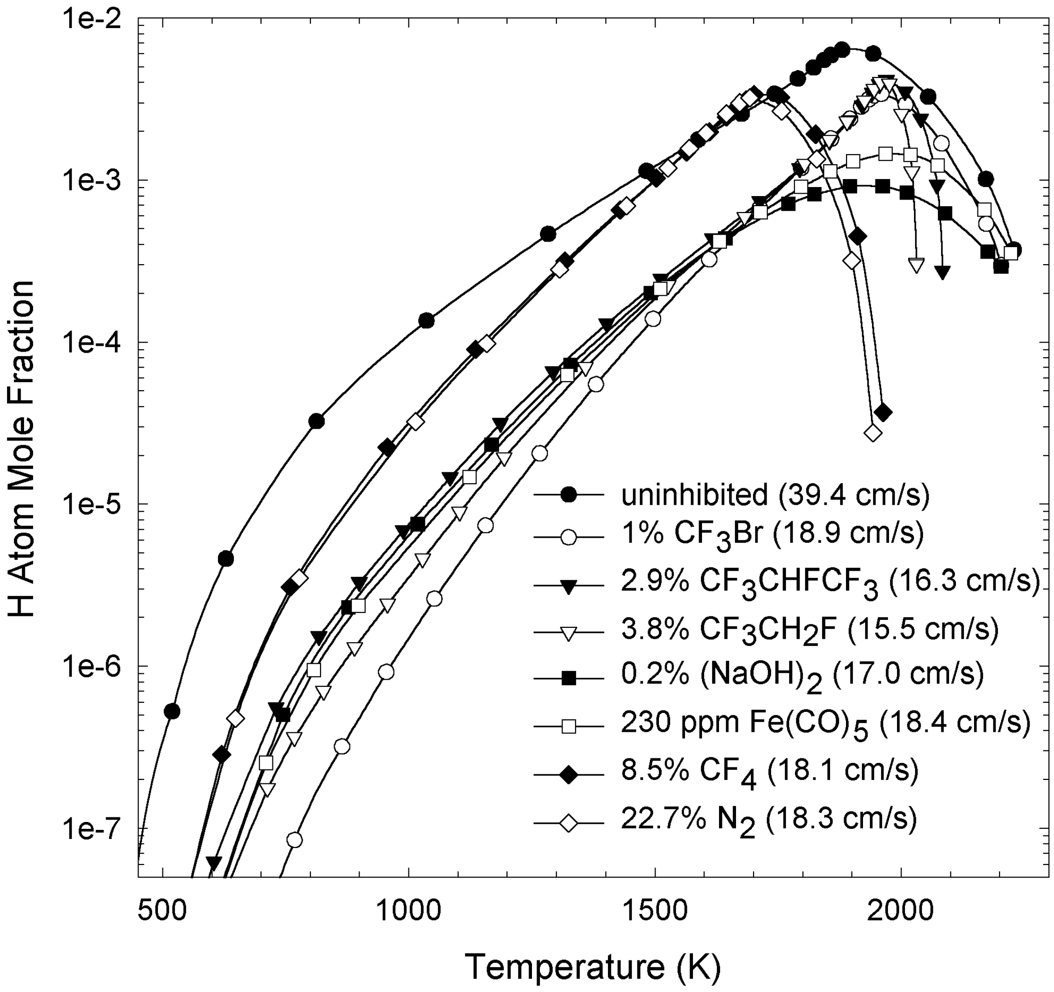

Figure 5: Mole fraction of atomic hydrogen as a function of local flame temperature for an uninhibited atmospheric pressure methane/air flame, and the same flame inhibited by the indicated suppression agents.

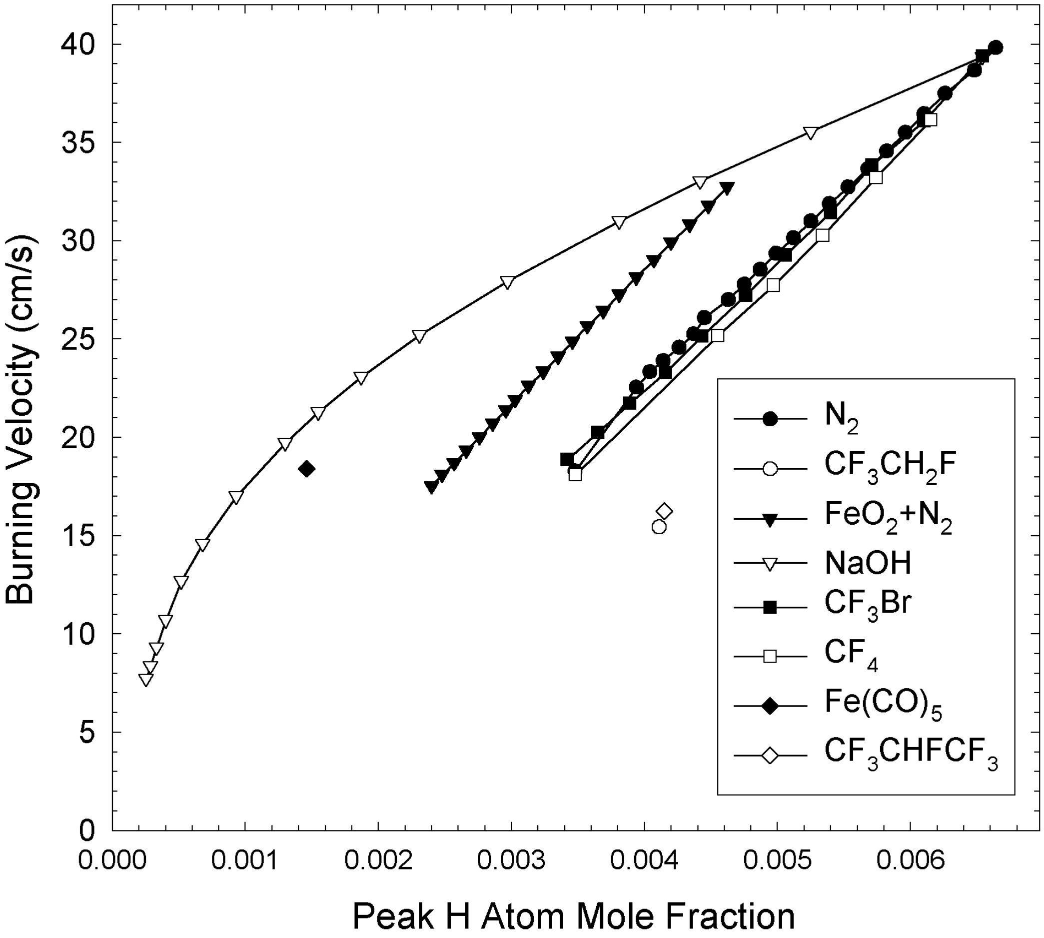

Figure 6: Relationship between burning velocity and peak concentration of atomic hydrogen for methane air flames inhibited by various compounds. The N_2 + Fe data is that presented in Figure 4, containing a FeO_2 as a reactant assumed to operate via an O + O inhibition cycle.

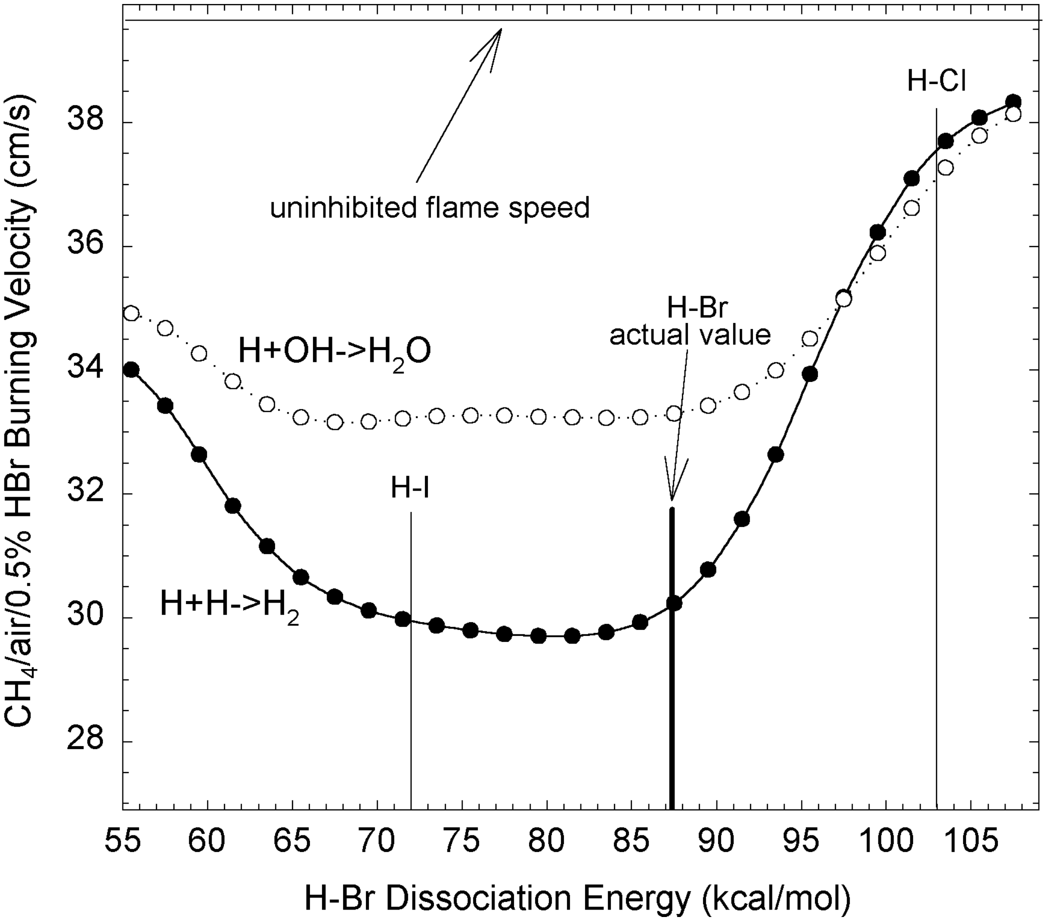

Figure 7: Calculated flame speed as a function of H-Br bond energy (see text) for premixed methane/air flames inhibited by 0.5% HBr using the H + H and H + OH scavenging cycles of Table 3. The accepted values for the bond energies of H-Br, H-Cl, and H-I are indicated by vertical lines.

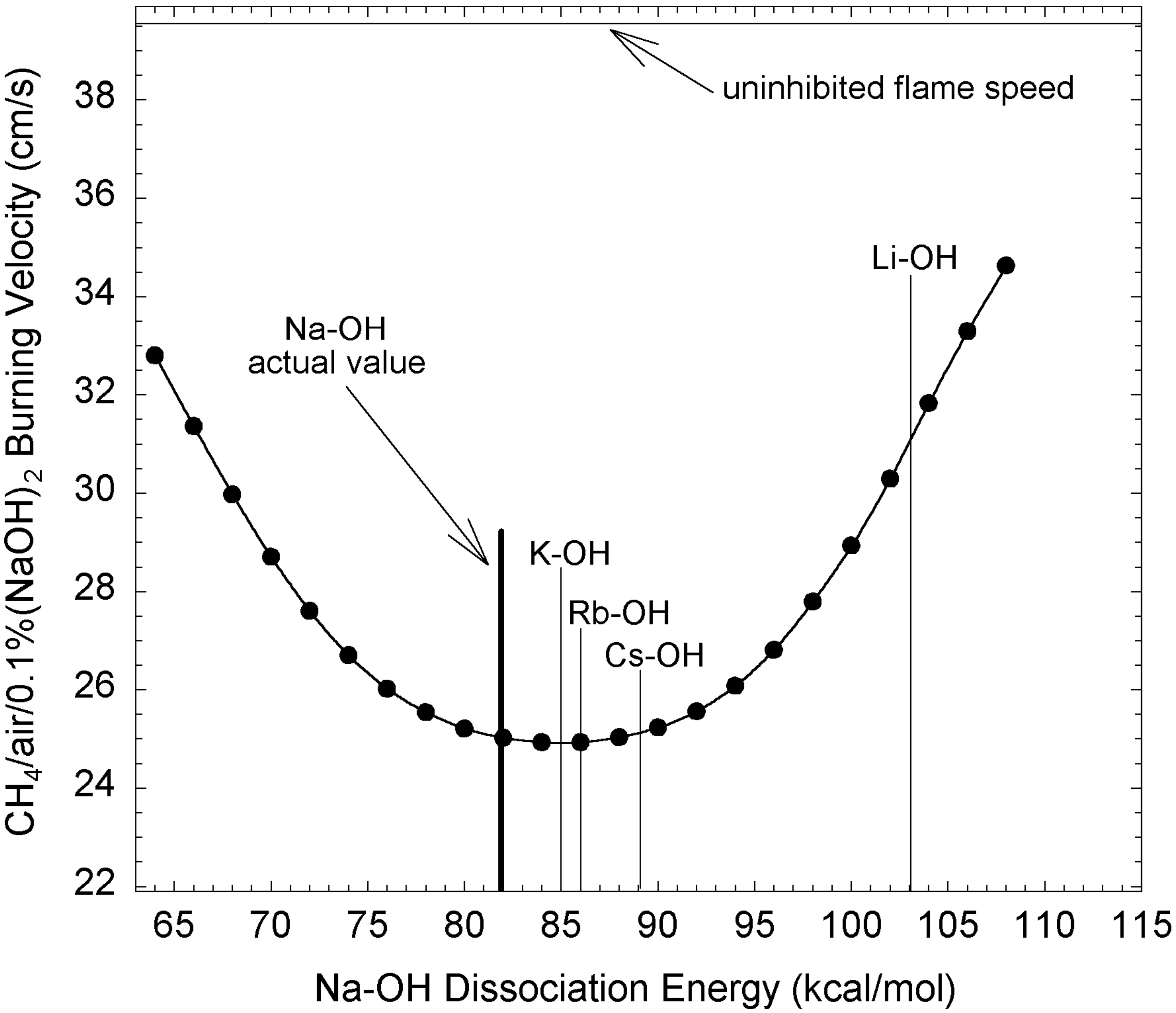

Figure 8: Calculated flame speed as a function of Na-OH bond energy (see text) for premixed methane/air flames inhibited by 0.1% $(NaOH)_2$ using the H + OH scavenging cycle of Table 3. The accepted values of X-OH bond energies for the alkali metals are indicated by vertical lines.

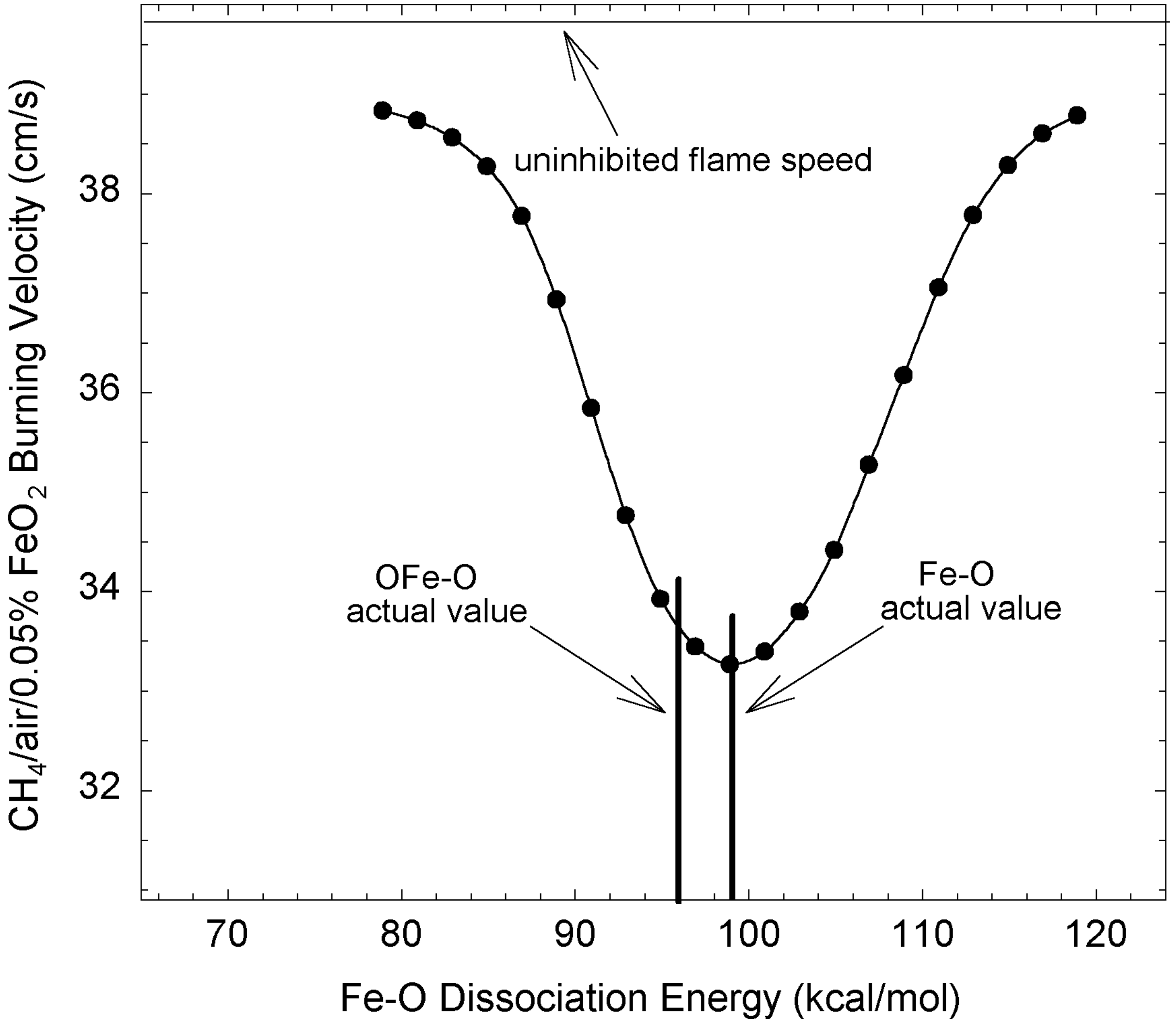

Figure 9. Calculated flame speed as a function of Fe-O bond energy (see text) for premixed methane/air flames inhibited by 500 ppm FeO_2 using the three step O + O scavenging cycle of Table 3. The accepted values of the Fe-O and OFe-O bond energies are indicated by vertical lines.